Z. Phys. C – Particles and Fields 29, 115–122 (1985)

Zeitschrift für Physik C Particles and Fields

Excited Lepton Production at LEP and HERA

K. Hagiwara[1], S. Komamiya[2], and D. Zeppenfeld[1]

1 Deutsches Elektronen-Synchrotron DESY, D-2000 Hamburg, Federal Republic of Germany
2 Physikalisches Institut der Universität, D-6900 Heidelberg, Federal Republic of Germany

Received 14 March 1985

Abstract. General expressions for single and pair production cross sections of excited leptons (e^*, μ^*, ν^*) are presented. Specific results are shown for a realistic $SU(2) \times U(1)$ invariant model. Pair production in e^+e^- annihilation can measure anomalous magnetic moments of excited leptons. Single production of e^* is dominated by the t-channel γ exchange contribution which makes its detection feasible up to masses just below the e^+e^- c.m. energy. Due to this small $|t|$ enhancement effect, contributions from elastic and resonance scattering in ep production of e^* are substantial. Realistic estimates of the excited lepton production cross section at HERA are given

I. Introduction

Composite models of quarks and leptons have attracted physicists for quite some time [1], because they have the potentiality of explaining the family problem and making the fermion masses and weak mixing angles calculable parameters. One clear signal for a composite structure of fermions would be the production of excited leptons or quarks, either pairwise, due to their normal gauge couplings, or singly, due to radiative transitions between normal and excited fermions. Searches for either mode have been performed in the past at PETRA [2], with negative results. This may have been expected since excited fermions should not be much lighter than the scale of compositeness, which according to present experimental constraints cannot be much lower than 1 TeV [3]. With the availability of higher center of mass energies in e^+e^- and ep collisions in the near future, the prospects for finding the lowest excited states of the spectrum become much better, if they exist at all. This has motivated us to reanalyze excited lepton production at LEP and HERA.

The highest excited lepton masses are accessible in single production searches. Excited electron (e^*) searches performed as a byproduct of analyzing radiative Bhabha scattering [2] are insensitive to e^* production at small scattering angles. The total production cross section, however, is completely dominated by very small angle scattering due to t-channel photon exchange. By identifying the $e\gamma$ decay products of e^* only, both of which typically have large transverse momentum of around $m_{e^*}/2$ about the beam axis, use can be made of this large cross section. We find that e^+e^- machines are in fact sensitive to e^* masses very close to the center of mass energy.

Similar results hold for ep collisions where a major part of the cross section is due to elastic and resonance scattering off the proton, while deep inelastic scattering gives a minor contribution to the full cross section at HERA energies.

The paper is organized as follows: in Sect. II we introduce the model and define the couplings to be used later. In Sect. III we give complete differential cross sections for single and pair production of excited leptons in e^+e^- collisions. For a number of representative cases we show total cross sections and demonstrate the effect of anomalous magnetic moments on pair production at both LEP I and LEP II energies. In Sect. IV we study the single production of e^* and ν_e^* at ep coliders. A general framework of exploiting low energy lepton production structure functions to evaluate the cross section is presented and some representative cross sections are shown. The last section is reserved to some concluding remarks.

II. Couplings and Models

We study the production of excited spin 1/2 fermions F assuming magnetic transitions to ordinary fermions f, which we describe by an effective Lagrangian of the form

$$\mathscr{L}_{\text{eff}} = \sum_{V=\gamma,Z,W^\pm} \frac{e}{\Lambda} \bar{F}\sigma^{\mu\nu}(c_{VFf} - d_{VFf}\gamma_5) f \partial_\mu V_\nu + \text{h.c.}. \tag{2.1}$$

We use the compositeness scale Λ instead of the excited fermion mass m_F for setting the scale of $\mathscr{L}_{\text{eff}}$: we see no reason why the magnetic transition couplings should be particularly large for small m_F. Although the compositeness scale should not be much smaller than 1 TeV [3], it could well be that the lowest mass of the excited fermion spectrum is somewhat lower than Λ. This is the possibility which can be tested at LEP and HERA.

There are several experimental bounds on the couplings c and d, the most stringent one being derived from $g-2$ measurements and the absence of electric dipole moments for the electron and muon [4]. To a high degree of accuracy $g-2$ measurements imply $|c_{\gamma Ff}|=|d_{\gamma Ff}|$ while the absence of electric dipole moments requires $c_{\gamma Ff}$ and $d_{\gamma Ff}$ to be relatively real if Λ is of the order of 1 TeV.

These constraints are a natural consequence of models which preserve $SU(2)\times U(1)$ invariance: since F_L and F_R must have the same $SU(2)\times U(1)$ quantum numbers (if a mass term is assumed prior to $SU(2)\times U(1)$ breaking, which can in fact be taken as the definition of an "excited" fermion in composite models with chiral protection) only one of them can couple to light fermions.

For the purpose of presenting results we choose a specific model [5] which greatly reduces the number of independent couplings. We assume that the excited electron and neutrino form a weak doublet

$$L=\begin{pmatrix}\nu_e^*\\ e^*\end{pmatrix} \tag{2.2}$$

which couples to the electron doublet

$$l_L=\begin{pmatrix}\nu_e\\ e\end{pmatrix}_L=\frac{1-\gamma_5}{2}\begin{pmatrix}\nu_e\\ e\end{pmatrix} \tag{2.3}$$

by the interaction Lagrangian

$$\mathscr{L}=\frac{gf}{\Lambda}\bar{L}\sigma^{\mu\nu}\frac{\vec{\tau}}{2}l_L\partial_\mu\vec{W}_\nu+\frac{g'f'}{\Lambda}\bar{L}\sigma^{\mu\nu}Yl_L\partial_\mu B_\nu+\text{h.c.}. \tag{2.4}$$

Here g and g' are the standard model $SU(2)$ and $U(1)$ coupling constants respectively, $\vec{\tau}$ denotes the Pauli matrices and $Y=-\frac{1}{2}$ is the hypercharge. In this model the coupling constants in (2.1) all satisfy $c_{VFf}=d_{VFf}$ and more specifically we have

$$\begin{aligned}
&c_{\gamma e^* e}=-\tfrac{1}{4}(f+f'),\\
&c_{\gamma\nu^*\nu}=\tfrac{1}{4}(f-f'),\\
&c_{Ze^*e}=-\tfrac{1}{4}(f\cot\theta_W-f'\tan\theta_W),\\
&c_{Z\nu^*\nu}=\tfrac{1}{4}(f\cot\theta_W+f'\tan\theta_W),\\
&c_{W^+\nu^* e}=c_{W^-e^*\nu}=\frac{f}{2\sqrt{2}\sin\theta_W}.
\end{aligned} \tag{2.5}$$

In the next section we compare single production with pair production of excited leptons. For the couplings of the gauge bosons to excited leptons we use the $SU(2)\times U(1)$ invariant Lagrangian

$$\begin{aligned}
\mathscr{L}=&g\bar{L}\frac{\vec{\tau}}{2}\left[\gamma^\mu\vec{W}_\mu+\frac{\kappa}{2m_L}\sigma^{\mu\nu}\partial_\mu\vec{W}_\nu\right]L\\
&+g'\bar{L}Y\left[\gamma^\mu B_\mu+\frac{\kappa'}{2m_L}\sigma^{\mu\nu}\partial_\mu B_\nu\right]L.
\end{aligned} \tag{2.6}$$

κ and κ' are the $SU(2)$ and $U(1)$ anomalous magnetic moments of the excited leptons respectively, which could in general be large*. In analogy to the Lagrangian (2.1) we obtain from (2.6)

$$\begin{aligned}
\mathscr{L}_{\text{eff}}=&\sum_{V=\gamma,Z}e\bar{F}\left[(A_{VF}+B_{VF}\gamma_5)\gamma^\mu V_\mu\right.\\
&\left.+\frac{\kappa_{VF}}{2m_F}\sigma^{\mu\nu}\partial_\mu V_\nu\right]F
\end{aligned} \tag{2.7}$$

with $B_{VF}=0$, since left and right components of the excited leptons are assumed to have the same $SU(2)\times U(1)$ quantum numbers, and

$$\begin{aligned}
&A_{\gamma e^*}=-1, \quad A_{Ze^*}=\frac{2\sin^2\theta_W-1}{2\sin\theta_W\cos\theta_W},\\
&A_{\gamma\nu^*}=0, \quad A_{Z\nu^*}=\frac{1}{2\sin\theta_W\cos\theta_W},
\end{aligned} \tag{2.8a}$$

$$\begin{aligned}
&\kappa_{\gamma e^*}=-\tfrac{1}{2}(\kappa+\kappa'), \quad \kappa_{Ze^*}=\tfrac{1}{2}(\kappa'\tan\theta_W-\kappa\cot\theta_W),\\
&\kappa_{\gamma\nu^*}=\tfrac{1}{2}(\kappa-\kappa'), \quad \kappa_{Z\nu^*}=\tfrac{1}{2}(\kappa'\tan\theta_W+\kappa\cot\theta_W).
\end{aligned} \tag{2.8b}$$

In order to specify the gauge couplings of normal leptons (f and f'), we use the following notation for the standard electroweak Lagrangian

$$\mathscr{L}_{SM}=\sum_{V=\gamma,Z,W^\pm}e\bar{f}'\gamma^\mu(a_{Vf'f}-b_{Vff'}\gamma_5)fV_\mu. \tag{2.9}$$

When presenting numerical results we always use the specific couplings of the model Lagrangians (2.4) and (2.6) and the standard model couplings for normal leptons. For all formulas, however, we use the more general notation introduced in (2.1), (2.7) and (2.9).

III. e^+e^- Collisions

Using the effective Lagrangians of the last section we now calculate the production cross-section for excited leptons to lowest order in $\alpha=e^2/4\pi$. Single production, i.e. the process $e\bar{e}\to F\bar{f}$ (F denotes the excited lepton and f is an ordinary light lepton) proceeds via the Feynman diagrams of Fig. 1 and the differential cross-section reads**

* Here we choose m_L rather than Λ to set the scale for the anomalous couplings so that they correspond to conventional anomalous magnetic moments

** For the special case of e^* production by photon exchange only, our result agrees with the formula given in [6] except for an overall normalization factor of 4

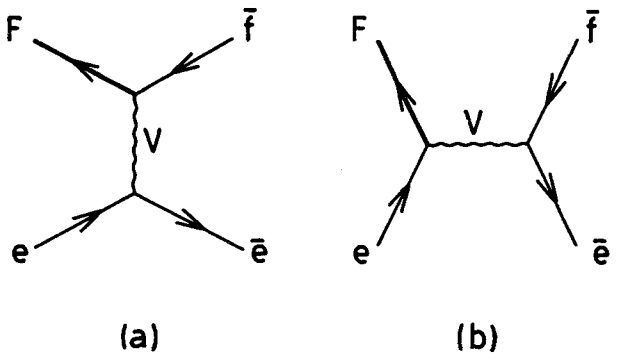

Fig. 1a and b. Feynman diagrams for the process $e\bar{e}\to F\bar{f}$. The excited fermion F is denoted by thick solid lines. Wavy lines correspond to $V=\gamma, Z$, or W

$$\frac{d\sigma}{dt}(e\bar{e}\to F\bar{f})=\frac{2\pi\alpha^2}{s^2\Lambda^2}\sum_{V,V'}\{s([m_F^2(s-m_F^2)+2tu]A_1 + m_F^2(t-u)A_2)D_V(s)D_{V'}(s)^* + stu\,\mathrm{Re}[(A_3^+ + A_3^-)D_V(s)D_{V'}(t)^*] + t([m_F^2(t-m_F^2)+2su]A_4 + m_F^2(s-u)A_5)D_V(t)D_{V'}(t)^* + \Delta_{VV'}\}. \tag{3.1}$$

Here s, t and u denote the usual Mandelstam variables, m_F is the mass of the excited lepton, and the sum over gauge bosons runs over γ, Z, and W. The gauge boson propagator factor is

$$D_V(q^2)=[q^2-m_V^2+im_V\Gamma_V\theta(q^2)]^{-1} \tag{3.2}$$

(θ being the step function) and the coefficients A_i can be expressed in terms of the coupling constants defined in the previous section as

$$\begin{aligned}
A_1&=(a_{Vee}a^*_{V'ee}+b_{Vee}b^*_{V'ee})\cdot(c_{VFf}c^*_{V'Ff}+d_{VFf}d^*_{V'Ff}),\\
A_2&=(a_{Vee}b^*_{V'ee}+b_{Vee}a^*_{V'ee})\cdot(c_{VFf}d^*_{V'Ff}+d_{VFf}c^*_{V'Ff}),\\
A_3^{\pm}&=(a_{Vee}\pm b_{Vee})(c_{VFf}\pm d_{VFf})\cdot(a^*_{V'ef}\pm b^*_{V'ef})(c^*_{V'Fe}\pm d^*_{V'Fe}),\\
A_4&=(a_{Vef}a^*_{V'ef}+b_{Vef}b^*_{V'ef})\cdot(c_{VFe}c^*_{V'Fe}+d_{VFe}d^*_{V'Fe}),\\
A_5&=(a_{Vef}b^*_{V'ef}+b_{Vef}a^*_{V'ef})\cdot(c_{VFe}d^*_{V'Fe}+d_{VFe}c^*_{V'Fe}).
\end{aligned} \tag{3.3}$$

In (3.1) terms proportional to light fermion masses have been neglected. This is a very good approximation except for e^* production via t-channel photon exchange, where a term proportional to m_e^2/t^2 should be added. This is achieved by setting

$$\Delta_{\gamma\gamma}=-m_e^2\frac{2m_F^4}{t^2}(|c_{\gamma e^*e}|^2+|d_{\gamma e^*e}|^2) \tag{3.4}$$

while for all other cases $\Delta_{VV'}$ can safely be neglected.

This additional term gives a finite contribution to the total cross-section in the $m_e\to 0$ limit since $t_{\min}$ is also proportional to m_e^2:

$$|t|_{\min}=m_e^2\frac{m_F^4}{s(s-m_F^2)}\left[1+O\left(\frac{m_e^2}{m_F^2}\right)\right]. \tag{3.5}$$

This low value of $t_{\min}$ implies that the e^* production cross-section, being a linear combination of $1/t$ and m_e^2/t^2, is extremely peaked in the forward direction. Most likely the accompanying e^+ will therefore be lost in the beam pipe, the signal for e^* production being its $e^-\gamma$ decay products.

The angular distribution of this electron photon pair is fairly flat. In the e^* rest frame with θ being the angle between incoming and outgoing electron we find at $t\approx 0$

$$\frac{d\Gamma}{d\cos\theta}\sim 1+\left(\frac{cd^*+c^*d}{|c|^2+|d|^2}\right)^2\cos\theta. \tag{3.6}$$

For $c=\pm d$, as implied by our model Lagrangian, this gives a $1+\cos\theta$ dependence. For $d=0$, as often used in the literature [2, 6], the angular distribution is flat. In either case, the transverse momentum of the final electron and photon with respect to the beam axis should exhibit a Jacobian peak at $m_{e^*}/2$. The $1+\cos\theta$ angular distribution predicted by models with chiral protection makes the final electron prefer the initial electron momentum direction; this is *opposite* to the angular distribution arising from the QED Compton process.

The $\bar{F}$ production cross-section is obtained by exchanging t and u in (3.1) when CP is conserved. In the following we show the F production cross-section only. For single production the total cross-section for both F and $\bar{F}$ is just double the rate presented in the figures.

The size of the t-channel enhancement can best be appreciated by comparing total cross-sections for e^* and μ^* production. In Fig. 2 we show total cross-sections for $\sqrt{s}=200$ GeV, corresponding to the proposed energy of LEP II, for a range of excited lepton masses*. For the couplings we choose $f/\Lambda=f'/\Lambda=(1\,\mathrm{TeV})^{-1}$ in this and all further plots**. e^* production is larger than μ^* production by two orders of magnitude! And most importantly the e^* cross-section remains large for m_{e^*} very close to the center of mass energy, even up to 199 GeV. The t-channel enhancement is also important for ν_e^* production via W exchange as can be seen by comparing the ν_e^* and ν_μ^* curves in Fig. 2.

Shown in Fig. 3 are the excited lepton production cross-sections in e^+e^- annihilation at $\sqrt{s}=93$ GeV

* In our numerical calculations we set $\alpha=1/128, \sin^2\theta_W=0.22$ $m_W=82$ GeV, $m_Z=93$ GeV and $\Gamma_Z=3$ GeV

** This value for f/Λ is quite conservative. Present limits from $g-2$ measurements [4] or e^* exchange in $e^+e^-\to\gamma\gamma$ [2] allow the cross-sections to be larger by two orders of magnitude or more

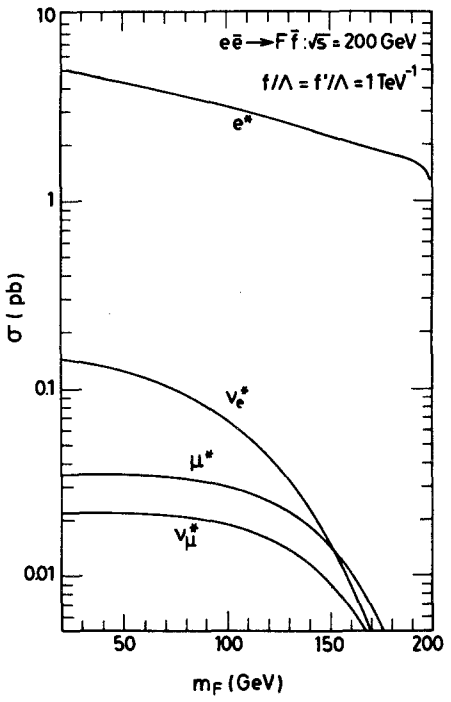

Fig. 2. Total production cross-section of excited fermions ($F = e^*, \mu^*, \nu_e^*$, and ν_μ^*) via the process $e\bar{e} \to F\bar{f}$ at $\sqrt{s} = 200\,\text{GeV}$. For the magnetic transition couplings, we take $f/\Lambda = f'/\Lambda = 1\,\text{TeV}^{-1}$

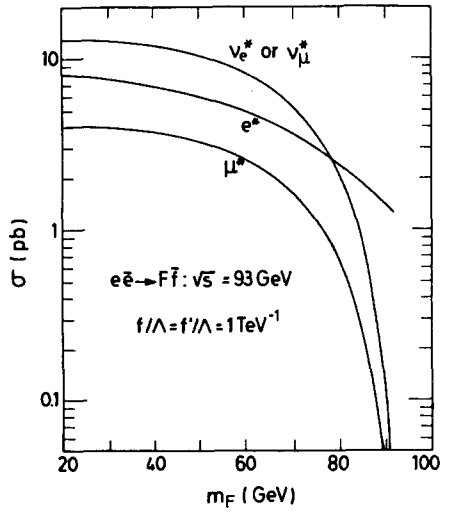

Fig. 3. Same as Fig. 2 at $\sqrt{s} = 93\,\text{GeV}\,(= m_Z)$

$(= m_Z)$. Even on top of the Z-peak, t-channel photon exchange gives a nonnegligible contribution to e^* production, especially for the high mass region. This is clearly seen in Fig. 3 by comparing the e^* and μ^* curves.

The cross-sections for single production should be compared to the pair production cross-section when $2m_F < \sqrt{s}$. Since excited fermions could have large

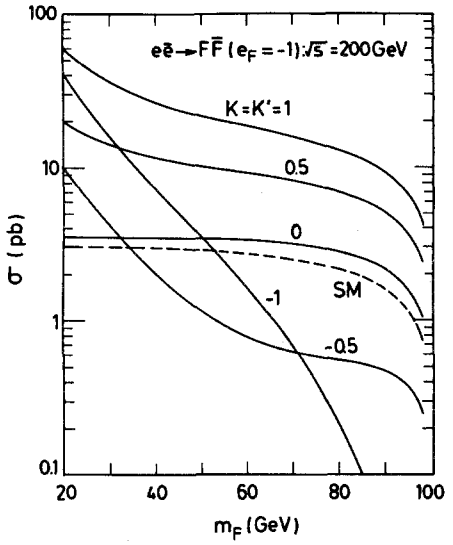

Fig. 4. Total pair production cross-section of excited charged fermions (e.g., μ^*) in e^+e^- annihilation at $\sqrt{s} = 200\,\text{GeV}$ for various values of anomalous magnetic moments κ and κ'. The standard sequential heavy lepton production cross-section is shown as a dashed line

anomalous magnetic moments, we include them by using the effective Lagrangian (2.7). The $F\bar{F}$ pair production cross-section in the center of mass frame is found to be

$$\frac{d\sigma(e\bar{e} \to F\bar{F})}{d\cos\theta} = \pi\alpha^2\beta s(B_0 + B_1\cos\theta + B_2\cos^2\theta), \tag{3.6}$$

where $\beta = \sqrt{1 - 4m_F^2/s}$ and θ is the polar angle between the electron beam direction and F. Leaving out the fermion indices, the coefficients B_i are expressed in terms of the coupling constants defined in the previous section, as

$$B_0 = \sum_{V,V'} D_V(s) D_{V'}(s)^* (a_V a_{V'}^* + b_V b_{V'}^*) \cdot \left[(A_V + \kappa_V)(A_{V'}^* + \kappa_{V'}^*) - \frac{\beta^2}{2}(A_V A_{V'}^* - B_V B_{V'}^*) - \frac{s}{4m_F^2}\kappa_V \kappa_{V'}^* \right],$$

$$B_1 = \beta \sum_{V,V'} D_V(s) D_{V'}(s)^* (a_V b_{V'}^* + b_V a_{V'}^*) \cdot [(A_V + \kappa_V) B_{V'}^* + B_V (A_{V'}^* + \kappa_{V'}^*)],$$

$$B_2 = \frac{\beta^2}{2} \sum_{V,V'} D_V(s) D_{V'}(s)^* (a_V a_{V'}^* + b_V b_{V'}^*) \cdot \left[A_V A_{V'}^* + B_V B_{V'}^* - \frac{s}{4m_F^2}\kappa_V \kappa_{V'}^* \right].$$

In Fig. 4 we show the resulting total cross-section at $\sqrt{s} = 200\,\text{GeV}$ for $\kappa = \kappa' = 0, \pm 0.5$ and ± 1 in the

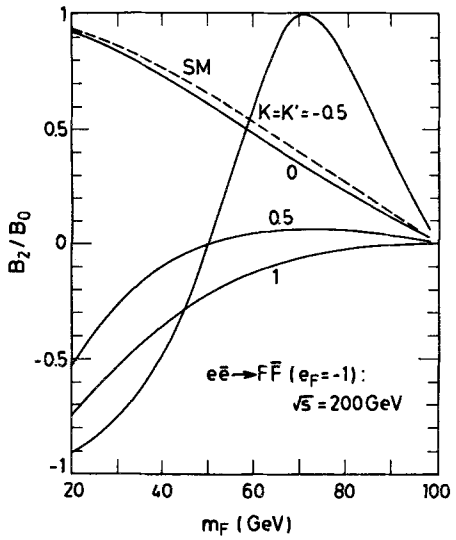

Fig. 5. Angular distribution parameter B_2/B_0 for pair production of excited charged leptons in e^+e^- annihilation at $\sqrt{s}=200\,\text{GeV}$ for various values of anomalous magnetic moments. The standard sequential heavy lepton case is again shown by a dash line

model Lagrangian (2.6). Several comments are in order:

i) For $s \gg m_F^2$ the cross-section is considerably enhanced by a large magnetic moment, as is to be expected from the dimension 5 operator in the effective Lagrangian (2.7). In general, however, we should expect all the excited fermion couplings (A, B and κ) to exhibit form factor damping at high energies. The rising cross-section for $m_F^2 \ll s$ observed in Fig. 4 is an artifact of our choice of large constant anomalous moments for very light ($m_F \ll \Lambda$) excited leptons.

ii) When $\kappa=-1$, $A_V=-\kappa_V$ and $B_V=0$ follow, and the cross-section is proportional to β^5 instead of the phase space factor which is linear in β. This dramatic suppression of the cross-section is clearly seen in the figure. Even when the situation is not as unfavorable, opposite signs of κ_V and A_V can lead to a considerable suppression of $F\bar{F}$ production near the threshold.

iii) The angular distributions may also be changed dramatically. Again for $\kappa=\kappa'=-1$, or $A_V+\kappa_V=0=B_V$, we obtain $d\sigma/d\cos\theta \sim 1-\cos^2\theta$, i.e. the angular distribution can be identical to that for scalar pair production.

iv) Since excited fermions should couple vectorially to W and Z bosons (see (2.6)), the coefficient B_1 always vanishes. We do not expect a forward–backward charge asymmetry for excited leptons.

In order to make point iii) more transparent we show the ratio B_2/B_0 for $\mu^*\bar{\mu}^*$ production at $\sqrt{s}=200\,\text{GeV}$ in Fig. 5. The curves correspond to different values of $\kappa=\kappa'$ in the model Lagrangian (2.6).

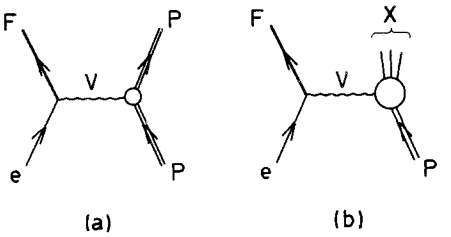

Fig. 6a and b. Schematic view of the excited lepton production process $ep\to Fp$ (**a**) and $ep\to F+$ anything (**b**). Wavy lines denote gauge bosons $V=\gamma, Z$, or W

IV. Single Production in *ep* Collisions

The e^+e^- cross-section (3.1) can easily be adapted to electron quark scattering: we only have to insert the appropriate couplings. For the deep inelastic contribution to the process $e^-p\to FX$ we thus obtain the integrated cross-section

$$\sigma(e^-p\to FX)=\int_{\hat{s}_{\min}/s}^{1}dx\int_{Q_0^2}^{sx-m_F^2}dQ^2\sum_q q(x,Q^2)\frac{d\hat{\sigma}}{dQ^2}\cdot(eq\to Fq';\hat{s}=sx) \tag{4.1}$$

in terms of the effective quark distribution $q(x,Q^2)$ in the proton and the parton cross-section*

$$\frac{d\hat{\sigma}}{dQ^2}(eq\to Fq')=\frac{2\pi\alpha^2}{\hat{s}^2\Lambda^2}Q^2\sum_{V,V'}\{[2\hat{s}^2-(Q^2+m_F^2)(2\hat{s}-m_F^2)]A_4\pm m_F^2(2\hat{s}-Q^2-m_F^2)A_5\}D_V(t)D_{V'}(t)^*. \tag{4.2}$$

The plus (minus) sign has to be taken for scattering off quarks (antiquarks), and the coefficients A_4 and A_5 can be expressed as before

$$A_4=(a_{Vq'q}a^*_{V'q'q}+b_{Vq'q}b^*_{V'q'q})(c_{VFe}c^*_{V'Fe}+d_{VFe}d^*_{V'Fe}),$$
$$A_5=(a_{Vq'q}b^*_{V'q'q}+b_{Vq'q}a^*_{V'q'q})(c_{VFe}d^*_{V'Fe}+d_{VFe}c^*_{V'Fe}), \tag{4.3}$$

for quarks (exchange subscripts q and q' for antiquarks).

When folding the parton cross-section with the quark distribution functions $q(x,Q^2)$, a low Q^2 cut Q_0^2 $\sim$ several GeV^2 must be applied in order to eliminate the phase space region where the parton model is not reliable any more. Q_0^2 slightly affects the x integration region via $\hat{s}_{\min}=m_F^2+Q_0^2$.

* Our formula for the process $eq\to e^*q$ agrees with the one obtained by Altarelli et al. [7] up to the sign of the γ–Z interference terms. By taking this into account, e.g. by switching the sign of the Z–e^*–e coupling, the curves presented in [7] are reproduced after proper rescaling of the couplings. e^* poduction at ep colliders has also been studied by Bagger and Peskin [8] in the equivalent photon approximation with a pointlike proton, which overestimates the elastic contribution at high e^* masses

Cutting away the low Q^2 region is a good approximation for ν_e^* production, where the only contribution comes from t-channel W exchange. For e^* production, however, a sizable contribution at low Q^2 is to be expected due to t-channel photon exchange. Because the parton model is unreliable in this region, we should use the experimental information on the electromagnetic structure function $F_1(x,Q^2)$ and $F_2(x,Q^2)$ of the proton directly. In terms of these functions the differential cross-section due to photon exchange (see Fig. 6) reads

$$\frac{d^2\sigma}{dW^2dQ^2}=\frac{\pi\alpha^2}{\Lambda^2}\frac{|c_{\gamma e^* e}|^2+|d_{\gamma e^* e}|^2}{(s-m_p^2)^2Q^4}\cdot\Bigg\{2F_1(x,Q^2)(2M^2-Q^2)(M^2+Q^2)+F_2(x,Q^2)\Bigg[\frac{4(s-m_p^2)^2Q^2}{W^2+Q^2-m_p^2}-(M^2+Q^2)\cdot\Bigg(4s-W^2-Q^2-3m_p^2+\frac{4m_p^2M^2}{W^2+Q^2-m_p^2}\Bigg)\Bigg]\Bigg\}. \tag{4.4}$$

M and m_p denote the e^* and the proton mass respectively, W is the invariant mass of the final hadron system, $Q^2=-t$, and $x=Q^2/(W^2+Q^2-m_p^2)$ as usual.

In order to evaluate the total e^* production cross section, we divide phase space into three regions, which we treat independently:

i) elastic region, i.e. elastic scattering off the proton: $W^2=m_p^2$, with no restriction on Q^2 apart from the kinematical one.

ii) low Q^2 region: $Q^2<Q_0^2$, $W^2>(m_p+m_\pi)^2$.

iii) deep inelastic region: $Q^2>Q_0^2$, $W^2>(m_p+m_\pi)^2$.

Regions i) and iii) are straightforward to handle. The deep inelastic contribution is given in (4.1). For the quark distribution functions we use the set I parametrization of Duke and Owens [9]. The elastic contribution i) as depicted in Fig. 6a is obtained by inserting the form factors

$$F_1(x,Q^2)|_{\text{elastic}}=\delta(W^2-m_p^2)\frac{Q^2}{2}G_M^2(Q^2),$$

$$F_2(x,Q^2)|_{\text{elastic}}=\delta(W^2-m_p^2)Q^2\cdot\Bigg[G_E^2(Q^2)+\frac{Q^2}{4m_p^2}G_M^2(Q^2)\Bigg]\cdot\Bigg(1+\frac{Q^2}{4m_p^2}\Bigg)^{-1} \tag{4.5}$$

into (4.4). We use the dipole fit for the electric and magnetic form factors G_E and G_M of the proton

$$G_E(Q^2)\approx G_M(Q^2)/2.79\approx[1+Q^2/0.71\,\text{GeV}^2]^{-2}. \tag{4.6}$$

For evaluating the contributions from the inelastic low Q^2 region ii) the optimal procedure would be to use directly the experimental data including the full resonance structure. An approximate calculation is sufficient for our purpose, however. We take the semilocal duality fit to the structure functions obtained by Brasse et al. [10] who exploited the rescaling variable of Rittenberg and Rubinstein [11].

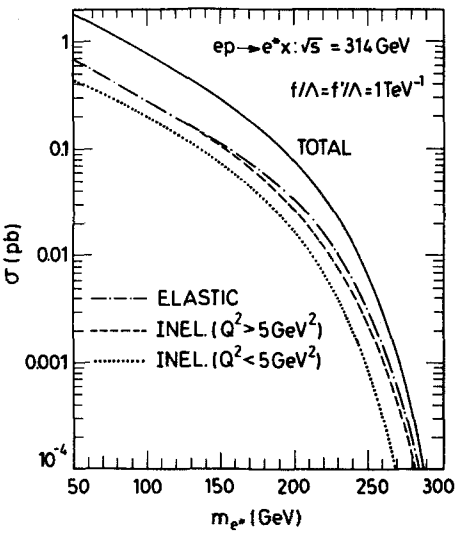

Fig. 7. Total e^* production cross-section versus e^* mass in ep collisions at $\sqrt{s}=314$ GeV with magnetic transition couplings $f/\Lambda=f'/\Lambda=1\ \text{TeV}^{-1}$. Elastic (dash-dotted line), inelastic low Q^2 (dotted line), and deep inelastic contributions (dashed line) are shown separately

In Fig. 7 we show the resulting e^* production cross-section for $Q_0^2=5\,\text{GeV}^2$ * at $\sqrt{s}=314\,\text{GeV}$. Again we choose $f/\Lambda=f'/\Lambda=(1\,\text{TeV})^{-1}$. The individual contributions of the three regions are shown separately in the figure. We find that due to t-channel enhancement the elastic cross-section is as large as or even larger than the deep inelastic contribution, and clearly low Q^2 dominates e^* production. This means that, even at HERA, the signal for e^* production will typically be a high p_T $e\gamma$ pair plus nothing, because with high probability the hadrons will be lost in the beam pipe. The absolute size of the signal completely depends on the values of f/Λ and f'/Λ which are realized in nature. We emphasize that the value $(1\,\text{TeV})^{-1}$, which we use, is highly arbitrary. Present experimental bounds on f/Λ [2, 4] allow cross-sections to be three to four orders of magnitude larger than the curves shown in the figures. Even when relaxing to $f/\Lambda\approx f'/\Lambda\approx m_{e^*}^{-1}$ only, experiments at HERA are able to detect excited electrons with masses as high as 250 GeV (at a rate of 11 events with an integrated luminosity of $100\,\text{pb}^{-1}$).

In Fig. 8 we show the total production cross-section of ν_e^* as compared to e^* in ep collisions at $\sqrt{s}=$

* For the low Q^2 parametrization of [10] we choose the one obtained by assuming $R=0.18$

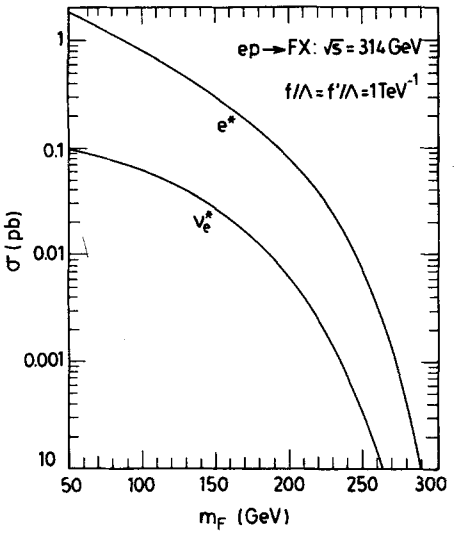

Fig. 8. Total production cross-section for e^* and ν_e^* versus their masses in ep collision at $\sqrt{s} = 314\,\text{GeV}$ with magnetic transition couplings $f/\Lambda = f'/\Lambda = 1\,\text{TeV}^{-1}$

314 GeV. Roughly speaking the ν_e^* production cross-section is one order of magnitude smaller than the e^* production rate for the range of accessible masses.

Finally, we remark that the total e^* production cross-section in Fig. 8 essentially is a function of $m_{e^*}/\sqrt{s}$ only, because the dominant contribution arises from photon exchange at low Q^2. The curve can be used for center of mass energies different from $\sqrt{s} = 314\,\text{GeV}$ by a simple rescaling of the e^* mass. We have checked that the resulting curve at $\sqrt{s} = 2\,\text{TeV}$ agrees to the exact calculation within 50%. The additional contribution at higher $\sqrt{s}$ is due to Z boson exchange which becomes more and more important as m_Z becomes negligible.

V. Conclusions

We have calculated complete differential cross-sections for single and pair production of excited leptons in e^+e^- and e^-p collisions. Interference between different gauge bosons, between s and t channel exchange, and between vector and tensor couplings in the case of pair production has been included. Our cross-sections are hence reliable for the full range of energies available in the near future including the vicinity of the Z-peak.

The largest signals are expected for single production of an excited electron in e^+e^- collisions when only the $e\gamma$ decay products of the e^* are required to be seen in the detector. This procedure allows the detection of excited electrons with masses almost as large as the center of mass energy of the colliding beams, even with fairly small magnetic couplings to normal electrons.

Prospects for ep collisions are not quite as good, but also there excited electrons with masses well above half the center of mass energy of the colliding beams can be detected for magnetic couplings of the order of $(1\,\text{TeV})^{-1}$.

Due to these large cross-sections we expect that excited electrons will probably first be seen in single production. Other excited leptons, if their mass is not too close to the compositeness scale, may first be detected in the pair production mode in e^+e^- annihilation. It should be noted, however, that the pair production cross-section can be quite different from the one of a fourth generation lepton if excited leptons possess large anomalous magnetic moments. Deviations should be particularly large close to threshold. The uncertainties in the couplings of excited leptons therefore forbid definite predictions for the production cross-sections in the case of pair production, even though the situation is not as uncertain as in single production, where the normalization of the cross-section is essentially a free parameter.

Finally we make brief comments on decay modes of excited leptons: In the $SU(2) \times U(1)$ model introduced in Sect. II we expect all the excited leptons to decay into their normal lepton partners and a photon below W and Z threshold except for very particular choices of the coupling constants f and f'. For example, if $f = f'$ exactly, the excited neutrinos cannot decay via photon emission. Instead they will decay via virtual W or Z emission giving final states similar to heavy sequential neutrinos. When excited fermion masses exceed W and Z masses, the branching fractions for various decay modes are determined by the couplings f and f' and phase space factors.

After essentially completing the present work we received a preprint by Courau and Kessler [12] where e^* production in e^+e^- collision has been studied in the equivalent photon approximation.

Acknowledgement. We thank R.D. Peccei for continuous interest in our work and for stimulating discussions. We thank M. Davier for making us aware of [12].

References

1. J.C. Pati, A. Salam: Phys. Rev.**D10**, 275 (1974); H. Terazawa, Y. Chikashige, K. Akama: Phys. Rev. **D15**, 480 (1977); H. Harari: Phys. Lett. **86B**, 83 (1979); M.A. Shupe: Phys. Lett. **86B**, 87 (1979); R. Casalbuoni, R. Gatto: Phys. Lett., **93B**, 47 (1980); H. Terazawa: Phys. Rev. **D22**, 184 (1980); H. Harari, N. Seiberg: Phys. Lett. **98B**, 269 (1981); O.W. Greenberg, J. Sucher: Phys. Lett. **99B**, 339 (1981); L. Abbott, E. Farhi: Nucl. Phys. **B189**, 547 (1981); H. Fritzsch, G. Mandelbaum: Phys. Lett. **102B**, 319 (1981); W. Buchmüler, S.T. Love, R.D. Peccei, T. Yanagida: Phys. Lett. **115B**, 233 (1982).
   For recent reviews and more complete list of references, see e.g., H. Terazawa: Proceedings of the Int. Conference on High Energy Physics, Leipzig, DDR (1984); H. Fritzsch, Lectures given at the International School on Subnuclear Physics, Erice, Sicily (August 1984), MPI report MPI-PAE/PTh 85/84 (1984)
2. CELLO Collab. H.J. Behrend et al.: Phys. Lett. **114B**, 287 (1982); JADE Collab. W. Bartel et al.: Z. Phys. C—Particles and Fields **19**, 197 (1983); ibid. C—Particles and Fields **24**, 223 (1984); TASSO Collab. M. Althoff et al.: DESY report 84-072 (1984); MARK-J Collab. B. Adeva et al.: MIT technical report # 141 (1984)

3. M.E. Peskin: Proceedings of the 1981 Intern. Symp. on Lepton and Photon Interactions at High Energies, pp. 880, eds. W. Pfeil et al. (Bonn, 1981), R. Barbieri, L. Maiani, R. Petronzio: Phys. Lett. **96B**, 63 (1980); S. Brodsky, S. Drell: Phys. Rev. **D22**, 2236 (1980); E. Eichten, K. Lane, M. Peskin: Phys. Rev. Lett. **50**, 811 (1983)
4. F.M. Renard: Phys. Lett. **116B**, 264 (1982); F. del Aguila, A. Méndez, R. Pascual: Phys. Lett. **140B**, 431 (1984); M. Suzuki: Phys. Lett. **143B**, 237 (1984)
5. F.M. Renard: Phys. Lett. **126B**, 59 (1983); **139B**, 449 (1984); N. Cabibbo, L. Maiani, Y. Srivastava: Phys. Lett. **139B**, 459 (1984); A. De Rújula, L. Maiani, R. Petronzio: Phys. Lett. **140B**, 253 (1984); J. Kühn, P. Zerwas: Phys. Lett. **147B**, 189 (1984)
6. H. Terazawa, M. Yasué, K. Akama, M. Hayashi: Phys. Lett. **112B**, 387 (1982)
7. G. Altarelli, B. Mele, R. Rückl: CERN report CERN-TH.3932/84 (1984)
8. J. Bagger, M.E. Peskin: SLAC report SLAC-PUB-3447 (1984)
9. D.W. Duke, J.F. Owens: Phys. Rev. **D30**, 49 (1984)
10. F.W. Brasse et al.: Nucl. Phys. **B39**, 421 (1972)
11. V. Rittenberg, H.R. Rubinstein: Phys. Lett. **35B**, 50 (1971); see also E.D. Bloom, F.J. Gilman: Phys. Rev. Lett. **25**, 1140 (1970)
12. A. Courau, P. Kessler: Orsay report, LAL/85-01 (1985)